

Investigation of Climate Effects on the Performance of Solar Chimney Power Plants Using Numerical and Analytical Models: A Case Study for Chlef, Algeria

Abstract. In this work, a semi-empirical model and 2D numerical model were developed to evaluate the Solar Chimney Power Plant (SCPP) efficiency in Chlef, Algeria. The airflow through the solar chimney is treated as a compressible flow in contrast to the Boussinesq model. In addition, the pressure and temperature in the solar are considered not constant. Thus, modelling was carried by means of Reynolds Averaged Navier-Stokes (RANS) equations coupled to the $k-\epsilon$ turbulence model. The meteorological parameters used in this study such as the temperature and the global solar radiation were measured in the Chlef region, Algeria, during 2018. The power output, updraft velocity and temperature were calculated and compared with the experimental results obtained from the Manzanares prototype to validate results of the compressible flow through the solar chimney obtained with the 2D numerical model are more accurate than those produced by Boussinesq model. The COMSOL Multiphysics software was used in this study to simulate the SCPP flow behaviour. Results demonstrate that the proposed numerical model derived from fundamental engineering calculations is reasonably accurate and can be effectively applied to investigate the SCPPs efficiency.

Streszczenie. Przedstawiono model solarnego kominowego źródła energii zaprojektowanego w Chlef – Algeria. Przepływ nagrzanego powietrza przez komin uruchamia turbinę wiatrową. Do opisu wykorzystano równania Reynolds Averaged Navier-Stokes. Do obliczeń wykorzystano typowe warunki atmosferyczne w Chlef. Symulację przeprowadzono wykorzystując oprogramowanie COMSOL Multiphysics. (Badania wpływu warunków klimatycznych na właściwości kominowego źródła solarnego na przykładzie obiektu w Chlef)

Keywords: Solar chimney power plant; Numerical model; compressible airflow; COMSOL Multiphysics.
Słowa kluczowe: solarne kominowe źródło energii, model numeryczny

Introduction

Since centuries, wind and solar power are among the important natural resources that mankind has always tried to exploit in the production, as these types of energies do not require complex or expensive technologies in terms of operation and use [1-2]. Today, the world is facing a growing global energy demand and unprecedented environment challenges reaches 37% in 2040 [3]. The energy landscape across the world is shifting away from the conventional fossil fuels towards the adoption of clean, renewable and environmental-friendly sources of energy [4-5]. Solar and wind energy are currently the dominant sources of clean renewable energy worldwide. Solar energy is used in two forms. The direct transformation of solar radiation into electricity, called solar photovoltaic energy, and the second form is solar thermal energy which uses the concept of solar radiation concentration to create high temperature intensity which can then be used to electricity production [6]. The SCPP is a relatively novel technology which uses solar thermal energy to generate electricity [7]. It is considered a cost-effective and promising solution which could potentially address the energy needs of developing countries. However, SCPPs can transform only a small fraction of the solar power obtained to electricity and therefore have a poor efficiency. This disadvantage is compensated by their robust and economical construction, and low maintenance costs [8].

The Solar Chimney Power Plant (SCPP), originally introduced by Professor J. Schlaich from Stuttgart University in the late 70's, includes collector roof, a tower and one or more turbines. The solar collector is usually covered by a plastic cover [9]. The solar insulation heats the air inside the collector; this creates a pressure difference between the inward and outward of the system, producing a continuous airflow movement from the solar collector to the middle of the collector and rises up through the chimney [10]. The chimney acts like a heat engine, which converts the heat produced from the collector into kinetic energy

which will then be converted into electric energy using a wind turbine-generator system [11].

The first experimental prototype of SCPP was constructed in 1982 in Manzanares (Spain) and was operated continuously till early 1989 as seen in figure 1. Field tests were carried out and the experimental data were published later [12]. The principles of the solar chimney system in the form of simple estimates were introduced by Haaf et al. [13].

SCPP prototype to validate the both models.



Fig. 1. Experimental prototype of SCPP in Manzanares, Spain

Due to the majority of simulation carried using of CFD fluent to analyze the enhanced performance of the solar chimney. Our research aims to develop a semi-empirical model and 2D numerical model in order to evaluate the

SCPP performance in Chlef region. For this purpose, the COMSOL Multiphysics software was used to simulate the behavior of the airflow in the SCPP where the airflow is treated as a compressible flow, the pressure and the temperature are considered not constant. The theoretically and numerically results are calculated and compared to the experimental findings of the Manzanares

Modeling of the solar chimney power plant

A standard SCPP structure is made up of three main components: a solar collector, a turbine connected a generator and tower [14]. As seen in figure 2, the SCPP functions in the presence of solar radiation and is characterized by a wide collector region that creates greenhouse effect, a long tower that promotes smooth fluid flow due to its chimney effect and one or two turbine-generator systems for electricity generation. The turbines should be placed under the chimney, where the airflow is important. In a SCPP structure, solar power is converted to thermal energy take place in the collector through the greenhouse effect. The chimney converts the generated thermal energy into kinetic energy and lastly a wind turbine connected with a generator converts this kinetic energy into electric power [15-16]. In this research a semi-empirical model and numerical model are developed to estimate the SCPP performance.

Semi-empirical model of the SCPP

In this section, the semi-empirical model is presented. The overall efficiency of the SCPP [17] is expressed by:

$$(1) \quad \eta_{SC} = \eta_{ch} \eta_{tg} \eta_c f_t$$

Where η_{ch} – chimney efficiency, η_{tg} – turbine generator efficiency, η_c – the collector efficiency, f_t – optimal drop ratio of turbine pressure and is given by:

$$(2) \quad f_t = \frac{2-m}{3}$$

The appropriate equation of m with ambient temperature T_a and the solar radiation G using in this work is used in this work is given by:

$$(3) \quad m = -18.8354 \times T_a^{-0.6143} \times G^{0.0504}$$

The SCPP efficiency is determined by the efficiency of each of the following components:

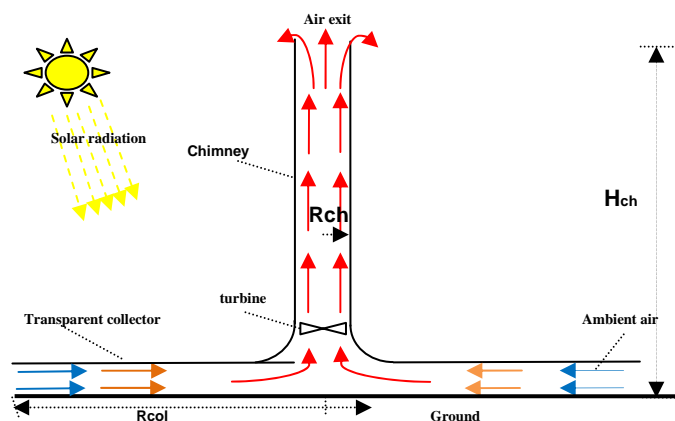


Fig.2. Schematic representation of Solar Chimney Power Plant used in this work.

Solar collector

The SCPP collector efficiency of [18] is obtained by:

$$(4) \quad \eta_c = \alpha - \frac{\beta \Delta T_0}{G}$$

where β – collector heat loss coefficient, α – collector's effective absorption coefficient within the range [0.75 to 0.8].

ΔT_0 – airflow temperature rise through the collector which is given by:

$$(5) \quad \Delta T_0 = T_0 - T_a$$

Where T_0 and T_a are collector outlet temperature, and ambient air temperature respectively.

Solar chimney

The chimney efficiency [18] is given by the Eq:

$$(6) \quad \eta_{ch} = \frac{H_{ch} \cdot g}{T_a \cdot C_p}$$

Where H_{ch} – chimney height, g – gravitational acceleration, and C_p – specific heat capacity. The maximum updraft velocity V_{ch} reached in the chimney is expressed as:

$$(7) \quad V_{ch} = \left(2 \cdot g \cdot H_{ch} \cdot \frac{\Delta T_0}{T_a}\right)^{1/2}$$

Wind turbine

Low speed vertical wind turbines were often used at the bottom of a solar chimney, where heated air forces transform up to 2/3 of the power in the flow to mechanical energy [19].

In this work, turbine generator efficiency is fixed at a value of 0.80 [17]. The total electrical power P_e of the solar chimney power plant is given as:

$$(8) \quad P_e = \eta_{SC} \cdot A_c \cdot G = f_t \cdot \eta_{ch} \cdot \eta_c \cdot A_c \cdot G \cdot \eta_{tg}$$

where A_c – collector area.

Numerical model of the SCPP

Computational fluid dynamics (CFD) is an effective method for discovering the best mechanical fluid systems modeling approach [20]. In this study, COMSOL Multiphysics software is used for the simulation of SCPP. Simulations are used by solving Reynolds-Averaged Navier-Stokes (RANS) equations to estimate the SCPP output. Domain grid is generated using the meshing tool COMSOL. The flow domain is calibrated for fluid dynamics with more concentrating element density on the outlet, junction regions and inlet. In this simulation, a triangular mesh composed of 12655 elements was used as depicted in Figure 3.

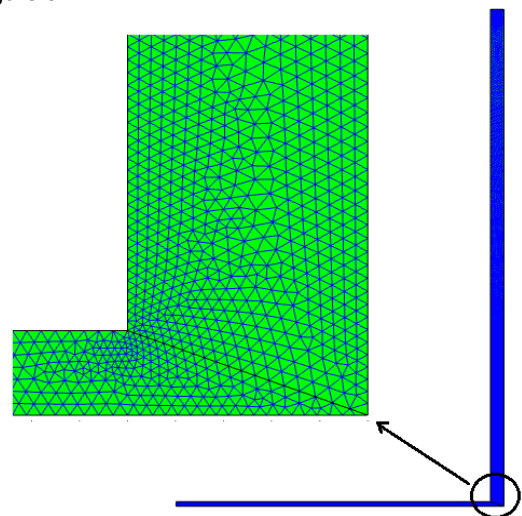


Fig.3. The 2-D meshing of the SCPP system.

Assumptions

To simplify the model used in the simulations the following assumptions are made:

- The system operates in steady state condition.
- 2D axisymmetric SCPP modeling.
- The wall of chimney is considered adiabatic.
- The effects due to wind fluctuations are neglected.
- The soil temperature at 1m deep of ground surface in the collector is constant.
- The properties of air outside the chimney can be supposed to be constant.

Governing equations

SCPP airflow is a type of flow powered by buoyancy, generally the intensity of which is defined through the Rayleigh number as:

$$(9) \quad R_a = \frac{g\beta\Delta TL^3\rho}{\mu\alpha} = Gr.Pr$$

Where L – mean height of collector, ΔT – mean airflow difference temperature in the system. The Rayleigh number of the Spanish SCPP prototype is clearly higher than 10^9 so the flow inside the system is considered as turbulent.

The governing steady airflow with conservation momentum, energy and mass equations is presented as: Continuity equation is as follow:

$$(10) \quad \frac{\partial\rho}{\partial t} + \nabla \cdot (\rho u) = 0$$

Momentum equation is as follow:

$$(11) \quad \rho \frac{\partial u}{\partial t} + \rho(u \cdot \nabla)u = \nabla[-P + (\mu + \mu_t)(\nabla u + (\nabla u)^T)] - \frac{2}{3}(\mu + \mu_t)(\nabla u) - \frac{2}{3}\rho kI + F$$

Energy equation is as follow:

$$(12) \quad \rho C_p \frac{\partial T}{\partial t} + \rho C_p u \cdot \nabla T = \nabla \cdot (K \nabla T) + Q + Q_{vh} + W_p$$

where F – volume forces, u – radial velocity, P – pressure and ρ – density.

The rate of dissipation ε and turbulence kinetic energy k are obtained as:

Turbulent kinetic energy equation is as follow:

$$(13) \quad \rho \frac{\partial k}{\partial t} + \rho(u \cdot \nabla)k = \nabla \cdot [(\mu + \frac{\mu_t}{\sigma_k})\nabla k] + P_k - \rho\varepsilon$$

Turbulent rate of dissipation equation is as follow:

$$(14) \quad \rho \frac{\partial \varepsilon}{\partial t} + \rho(u \cdot \nabla)\varepsilon = \nabla \cdot [(\mu + \frac{\mu_t}{\sigma_\varepsilon})\nabla \varepsilon] + C_{\varepsilon 1} \frac{\varepsilon}{k} P_k - C_{\varepsilon 2} \rho \frac{\varepsilon^2}{k}$$

Where $\mu_t = \rho C_\mu \frac{k^2}{\varepsilon}$ is the turbulent viscosity and

$\varepsilon = C_{\varepsilon 1} \frac{k^{3/2}}{L_T}$ is the energy dissipation.

The constants values used in the above equations for the turbulent model are: $C_\mu = 0.09$, $\sigma_k = 1$, $\sigma_\varepsilon = 1.3$, $C_{\varepsilon 1} = 1.44$ and $C_{\varepsilon 2} = 1.92$.

P_k Refers to the generation of turbulent kinetic energy caused by mean gradients of velocity and is given by:

$$(15) \quad P_k = \mu_t [\nabla u : (\nabla u + (\nabla u)^T)] - \frac{2}{3}(\nabla u)^2 - \frac{2}{3}\rho k \nabla u$$

Boundary conditions

The boundary conditions used are described from the data of weather related to the of Chlef area location, where the solar irradiation and ambient temperature are taken for a typical day of the year. The main computational domain boundary conditions are summarized in Table 1.

Table 1. Main boundary conditions

Surface	Boundary condition	Value
inlet	Inlet pressure	$P_i = P_{atm}, T_i = T_a$
outlet	Outlet pressure	$P_o = P_{atm}$
collector	Semi-transparent wall	$h = 5W/m^2 k$
Chimney wall	Insulated wall	$\frac{\partial T}{\partial r} = 0, u=0, v=0$
Ground	wall	$T = 307K$

Results and discussion

In this section, Simulations that integrate ambient temperature and solar radiation for the Chlef area are performed using the Manzanares prototype to examine the electrical energy produced by the SCPP system. Table 2 lists the principal dimensions of the Manzanares prototype which is used as the physical model.

Table 2. Main dimensions of the Manzanares SCPP prototype

parameter	Value[m]
Radius of collector	122
Radius of chimney	5.08
Height of collector	1.85
Height of chimney	194.6

Climatic parameters measurement

The geographical coordinates of the data collection site of Chlef region are $23^\circ 1'$ W Longitude, $36^\circ 23'$ N Latitude and 143 m altitude above sea level. The climatic parameters as ambient temperature and solar radiation are recorded by the "Vantage Pro 2" weather station at Chlef University Campus located in the town of Ouled Fares from January 1, 2018. Figure 4 indicates variance of the June 21st, 2018 measured ambient temperature and solar radiation. It shows that the ambient air temperature ranges from $20^\circ C$ to $31^\circ C$, while after sunrise the solar irradiance rises and reaches a maximum value of $894 W/m^2$ at 13:00 pm.

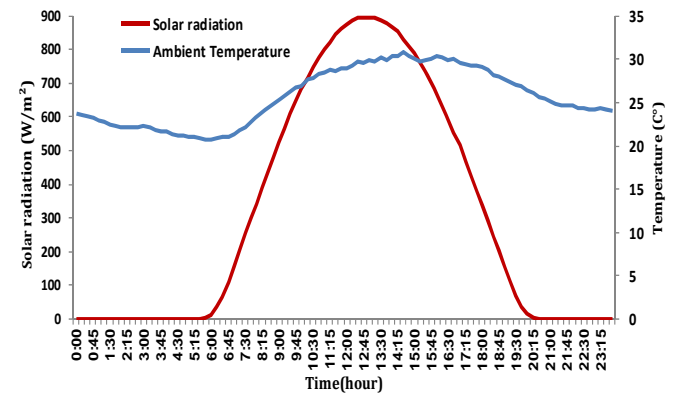


Fig.4. Variation of ambient air temperature and solar radiation in Chlef for the 21st June 2018.

Numerical and semi-empirical models validation

In this validation study, the numerical and the semi-empirical models are compared with the Manzanares prototype experimental data; where the results are presented in Fig 5-6 and 7.

Figure 5 presents the variation of the output power of the CFD model, analytical model, Boussinesq model ref [17] and the experimental results according to the global solar radiation intensity. It is observed that the numerical results are very close to the experimental results, while the

analytical results are a little far from them. It can be concluded that proposed model is more accurate than Boussinesq model used by ref [17]. Also in Figure 6, illustrates the variation of experimental data, CFD and ref [14] results of updraft velocity at the chimney inlet with solar radiation. The numerical results are very close to the experimental results, which indicates that the numerical results of our model are more accurate to those from ref [14-17] using the Boussinesq model. From these results it is clear, that the Both Figures 5 and 6 indicates a good agreement between the numerical and experimental results.

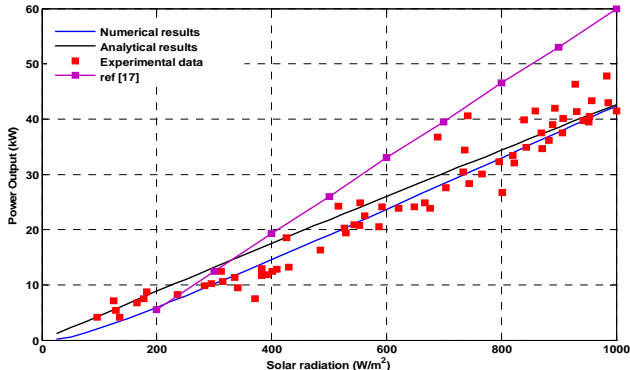


Fig.5. Validation of the output power results.

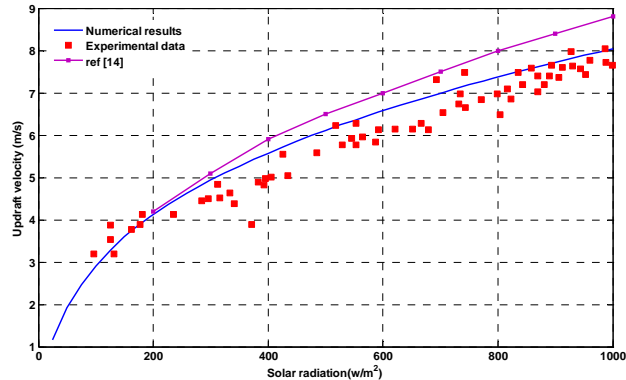


Fig. 6. Validation of the air velocity in the chimney

Figure 7 shows a comparison of the experimental and numerical data of the temperature in the collector and the difference between the collector surface and the ambient air. It can be observed that the experimental data are very consistent with the CFD results from 7:00 am to 24:00 pm. The gap between the CFD and experimental results from 24:00 pm to 7:00 am is much spaced because the solar irradiation is taken null in the CFD model.

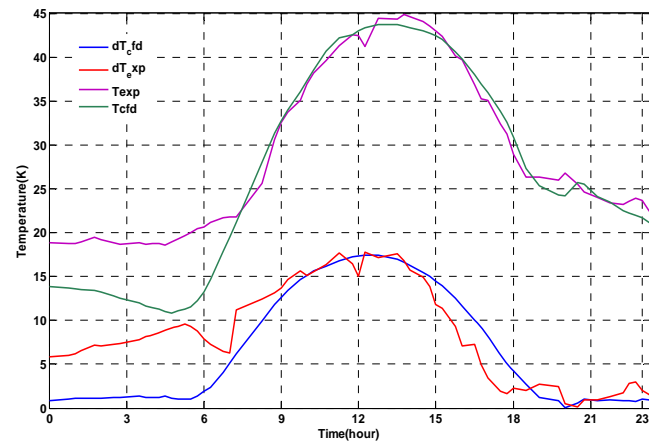


Fig.7. Validation of the air temperature rise and the air temperature in the collector.

The comparison between these results confirms that the numerical method adopted is a suitable approach for engineering calculations and can be used to investigate the performance of SCPPs.

Velocity magnitude, temperature contours

The distribution contour of air velocity magnitude within the SCPP system is shown in Figure 8. The maximum velocity is found at the base of the chimney where the turbine is mounted while it is very low in the collector and gradually rises to a maximum value of 13.93 m/s.

Figure 9 indicates the temperature distribution of air within the SCPP device. The minimum temperature values are found at the collector's entry, and then it gradually increases to a maximum value in the collector's centre at 316.61K.

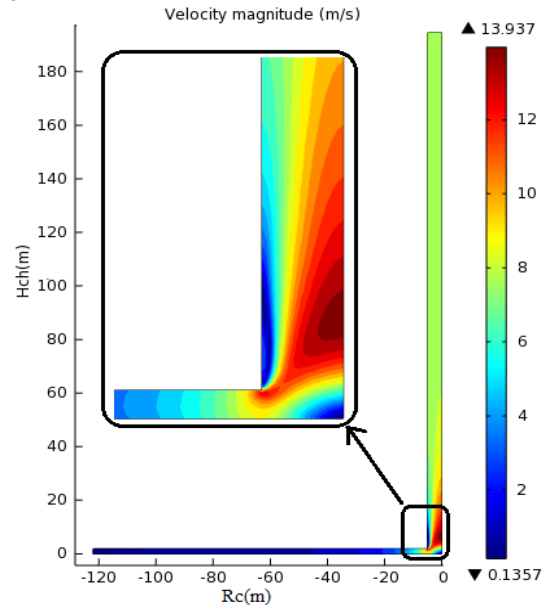


Fig.8. Velocity contours of air inside the SCPP

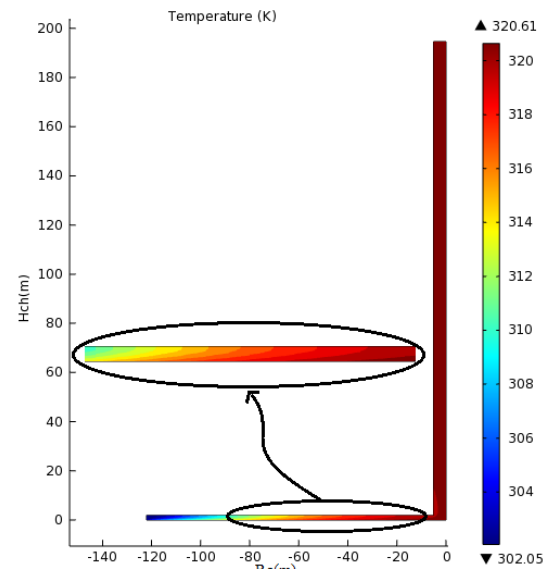


Fig.9. Temperature contours of air inside the SCPP

Effect of climatic factors on temperature rise and the updraft velocity

The variation in air temperature causes a disparity in density, which contributes to air flow. Air velocity is a measure of the flow speed. According to the time of the day of the 21st of June 2018, the hourly variance of the updraft velocity and temperature increase with solar radiation

intensity is shown in figure 10. It can be noted that the two plots follow the same trend of solar radiation. Besides, as the solar radiation rises at 893 w/m^2 both updraft velocity and the temperature rise reaches a maximum value of 13.94 m/s and 17.45°C respectively at 13:00pm. Based to these observations, it is clear that the updraft velocity and temperature rise are closely linked to solar radiation.

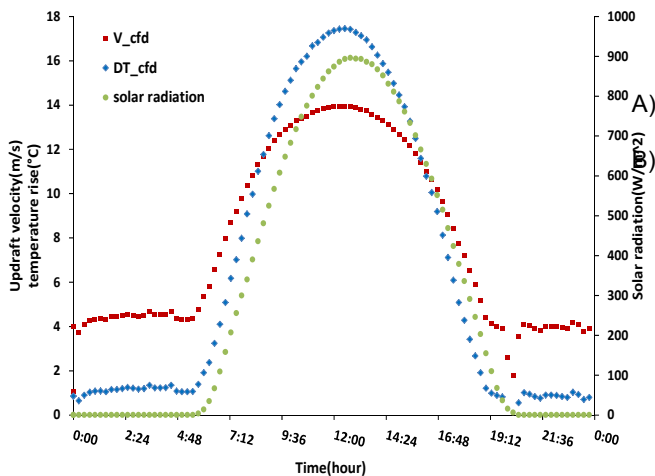


Fig.10. The hourly variation of temperature rise and updraft velocity with solar radiation

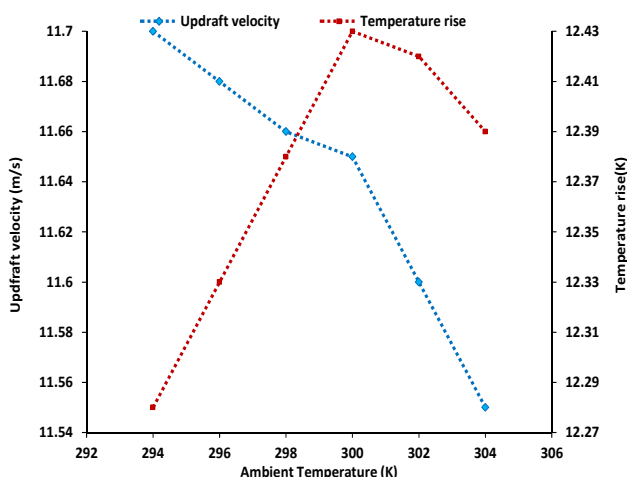


Fig.11. Ambient temperature effects on temperature rise and updraft velocity

Figure 11 shows the impacts of ambient temperature on updraft velocity and temperature rise in the chimney. The variation of ambient temperature has an apparent effect on updraft velocity while has not very apparent effect on temperature rise. Updraft speed decreases with higher ambient temperature, while temperature rise increases marginally with higher ambient temperature and declines marginally after a certain point.

Conclusion

This paper has discussed the modeling, simulation and experimental validation of solar chimney power plants for the region of Chlef in Algeria. To this end, two models have been proposed to describe the solar chimney dynamics using the numerical and analytical approaches. The COMSOL Multiphysics software was used in this study to simulate the SSCP system. In the CFD model, the airflow is treated as a compressible flow through the solar chimney and the pressure and the temperature are considered not

constant in the models. The output power, updraft velocity and temperature calculated analytically and numerically and compared with the experimental results of the SSCP prototype of Manzanares to validate both models. From this study, we can conclude the following:

- The numerical and semi-empirical models are very accurate compared to the model of ref [14-17] which is based on the Boussinesq model.
- The COMSOL Multiphysics software seems to be a good simulation tool for studying the thermodynamic behavior of the fluid in the solar chimney.
- The updraft velocity and temperature rise are closely linked to solar radiation
- the ambient air temperature has negligible impact on temperature increases while has an apparent impact on the air velocity
- The study confirms that the solar chimney is a potentially viable technology for the generation of electricity in the Chlef region.

As future work, we project to design and implement an agricultural multi-cell greenhouse with a solar chimney technology in the Chlef region using the existing greenhouses. For this, a simulation study of a combination of an agricultural multi-cell greenhouse with a solar chimney in Chlef region is being carried out. A comprehensive study is being conducted to investigate the power rating and scaling-up of the solar chimney to respond to the electric power demand and the ventilation of the multi-cell greenhouse.

Authors

Hadda. NOUAR, Department of Electrical Engineering, Hassiba Benbouali University, Chlef, 02000, Algeria. Email: h.nouar@univ-chlef.dz; Toufik. TAHRI, Department of Electrical Engineering, Hassiba Benbouali University, Chlef, 02000, Algeria. Email: t.tahri@univ-chlef.dz; Djilali. BENYOUCEF, Department of Electrical Engineering, Hassiba Benbouali University, Chlef, 02000, Algeria. Email: ben_plasma@yahoo.fr; Younes. CHAIBA, Department of Mechanical Engineering, Yahia Fares University, Medea, Algeria, Email: chibayounes@gmail.com; Mouloud. DENAI, University of Hertfordshire, Hatfield, Hertfordshire, United Kingdom, Email: m.denai@herts.ac.uk; Abdelghani. AZIZI, Department of Mechanical Engineering, Hassiba Benbouali University, Chlef, 02000, Algeria, Email: a.azizi@univ-chlef.dz

REFERENCES

- [1] Najm O.A., Shaaban S., Numerical investigation and optimization of the solar chimney collector performance and power density, *Energy Conversion and Management*, 168(2018), 150-161.
- [2] Aggad, F., Allaoui, T., Tamer, A., Denai, M., Modeling, Design and Energy Management of a Residential Standalone Photovoltaic-Fuel Cell Power System, *Przeglad Elektrotechniczny*, 96(2020), nr 8, 79-87.
- [3] Manjang, S., Rahman, Y. A., Distributed photovoltaic integration as complementary energy: consideration of solutions for power loss and load demand growth problems, *Przeglad Elektrotechniczny*, 96(2020), nr 9, 56-61.
- [4] Li B. X., P, Chan C., Application of phase change materials for thermal energy storage in concentrated solar thermal power plants: a review to recent developments, *Applied Energy*, 160(2015), 286-307.
- [5] Azizi A., Tahri T., Sellami M.H., Segni L., Belakroum R., Loudiyi K., Experimental and CFD investigation of small-scale solar chimney for power generation. Case study: southeast of Algeria, *Desalination and Water Treatment*, 160(2019), 1-8.
- [6] Amudam Y., Chandramohan V.P., Influence of thermal energy storage system on flow and performance parameters of solar updraft tower power plant: a three dimensional numerical analysis, *Journal of Cleaner Production*, 207(2019), 136-152.
- [7] Shuia E.M., Abuashe I.A., Arebi B.H., Experimental and Theoretical Investigation of Performance of a Solar Chimney Model, Part I: Experimental Investigation, *Solar Energy and Sustainable Development*, 3(2014), No. 1, pp. 51-62.

- [8] Koonsrisuk A., Chitsomboon T., Mathematical modeling of solar chimney power plants, *Energy*, 51(2013), 314-322.
- [9] Mullett L.B., The solar chimney- Overall efficiency, design and performance, *International journal of ambient energy*, 8(1987), No.1, 35-40.
- [10] Zou Z., He S., Modeling and characteristics analysis of hybrid cooling-tower-solar-chimney system, *Energy Conversion and Management*, 95(2015), 59-68.
- [11] Muhammed H.A., Atrooshi S.A., Modeling solar chimney for geometry optimization, *Renewable Energy*, 138(2019), 212-223.
- [12] Elwekeel F.N., Abdala A.M., Rahman M.M., Effects of novel collector roof on solar chimney power plant performance, *Journal of Solar Energy Engineering*, 141(2012), No. 3.
- [13] Haaf W., Friedrich K., Mayr G., Schlaich J., Solar chimneys part I: principle and construction of the pilot plant in Manzanares, *International Journal of Solar Energy*, 2(1983), No. 1, pp. 3-20.
- [14] Guo P., Li J., Wang Y., Numerical simulations of solar chimney power plant with radiation model, *Renewable energy*, 62(2014), 24-30.
- [15] Rabehi R., Chaker A., Aouachria Z., Tingzhen M., CFD analysis on the performance of a solar chimney power plant system: Case study in Algeria, *International Journal of Green Energy*, 14(2017), No. 12, 971-982.
- [16] Al Alawin A., Badran O., Awad A., Abdelhadi Y., Al-Mofleh A., Feasibility study of a solar chimney power plant in Jordan, *Applied Solar Energy*, 48(2012), No. 4, 260-265.
- [17] Guo P., Li J., Wang Y., Evaluation of the optimal turbine pressure drop ratio for a solar chimney power plant, *Energy Conversion and Management*, 108(2016), 14-22.
- [18] Shariatzadeh O.J., Refahi A.H., Abolhassani S.S., Rahmani M., Modeling and optimization of a novel solar chimney cogeneration power plant combined with solid oxide electrolysis/fuel cell, *Energy Conversion and Management*, 105(2015), 4.
- [19] Lal S., Kaushik S.C., Hans R., Experimental investigation and CFD simulation studies of a laboratory scale solar chimney for power generation, *Sustainable Energy Technologies and Assessments*, 13(2016), 13-22.
- [20] Ayadi A., Nasraoui H., Bouabidi A., Driss Z., Bsisa M., Abid M.S., Effect of the turbulence model on the simulation of the air flow in a solar chimney, *International journal of thermal sciences*, 130(2018), 423-434.